

# Structural Refinements and Thermal Properties of L(+)-Tartaric, D(-)-Tartaric, and Monohydrate Racemic Tartaric Acid

Takanori Fukami<sup>1</sup>, Shuta Tahara<sup>1</sup>, Chitoshi Yasuda<sup>1</sup>, Keiko Nakasone<sup>1</sup>

<sup>1</sup>Department of Physics and Earth Sciences, Faculty of Science, University of the Ryukyus, Japan

Correspondence: Takanori Fukami, Department of Physics and Earth Sciences, Faculty of Science, University of the Ryukyus, Okinawa 903-0213, Japan. Tel: 81-98-895-8509. E-mail: fukami@sci.u-ryukyu.ac.jp

Received: February 15, 2016 Accepted: March 2, 2016 Online Published: March 10, 2016

doi:10.5539/ijc.v8n2p9

URL: <http://dx.doi.org/10.5539/ijc.v8n2p9>

## Abstract

Differential scanning calorimetry, thermogravimetric-differential thermal analysis, and X-ray diffraction measurements were performed on single crystals of L(+)-tartaric, D(-)-tartaric, and monohydrate racemic (MDL-) tartaric acid. The exact crystal structures of the three acids, including the positions of all hydrogen atoms, were determined at room temperature. It was pointed out that one of O–H–O hydrogen bonds in MDL-tartaric acid has an asymmetric double-minimum potential well along the coordinate of proton motion. The weight losses due to thermal decomposition of L- and D-tartaric acid were observed to occur at 443.0 and 443.2 K, respectively, and at 306.1 and 480.6 K for MDL-tartaric acid. The weight losses for L- and D-tartaric acid during decomposition were probably caused by the evolution of 3H<sub>2</sub>O and 3CO gases. By considering proton transfer between two possible sites in the hydrogen bond, we concluded that the weight losses at 306.1 and 480.6 K for MDL-tartaric acid were caused by the evaporation of half the bound water molecules in the sample, and by the evaporation of the remaining water molecules and the evolution of 3H<sub>2</sub>O and 3CO gases, respectively.

**Keywords:** tartaric acid C<sub>4</sub>H<sub>6</sub>O<sub>6</sub>, monohydrate racemic tartaric acid C<sub>4</sub>H<sub>6</sub>O<sub>6</sub>·H<sub>2</sub>O, double-minimum potential, thermal decomposition, DSC, TG-DTA, X-ray diffraction

## 1. Introduction

Tartaric acid (chemical formula: C<sub>4</sub>H<sub>6</sub>O<sub>6</sub>; systematic name: 2,3-dihydroxybutanedioic acid) is found in grapes, currants, gooseberries, oranges, apples, and in most acidulous fruits, and is widely used in food, medicine, chemistry, light industry, etc. Many tartrate compounds are formed by the reaction of tartaric acid with various positive ions and are used in numerous industrial applications for transducers and in linear and non-linear mechanical devices due to their excellent dielectric, ferroelectric, piezoelectric, and nonlinear optical properties (Abdel-Kader et al., 1991; Desai & Patel, 1988; Firdous et al., 2010; Torres et al., 2002). Several types of tartaric acid crystals, such as potassium hydrogen tartrate, KC<sub>4</sub>H<sub>5</sub>O<sub>6</sub>, and calcium tartrate, CaC<sub>4</sub>H<sub>4</sub>O<sub>6</sub>, develop naturally in bottled wine and are the major cause of wine's natural and harmless sediment (Boese & Heinemann, 1993; Buschmann & Luger, 1985; Derewenda, 2008; Hawthorne et al., 1982). The sediment of tartrate crystals is a by-product of the wine industry and has to be removed from the wine after yeast fermentation of the grape juice.

Tartaric acid has two asymmetric carbon atoms in a molecule, which provides for four possible different forms: L(+)-tartaric, D(-)-tartaric, racemic (DL-) tartaric, and meso-tartaric acid (Bootsma & Schoone, 1967; Derewenda, 2008; Nie et al., 2001; Okaya et al., 1966; Parry, 1951; Song et al., 2006; Stern & Beevers, 1950). The most common form in nature is L-tartaric acid; meso-tartaric acid is human-made and does not occur in nature. Solutions of L- and D-tartaric acid rotate the plane of polarized light to the left and to the right, respectively, whereas of DL- and meso-tartaric acid show no rotation of plane-polarized light. These properties of optically active molecules derived from tartaric acid were discovered by Biot (Lowry, 1923). Louis Pasteur first separated the two enantiomers of sodium ammonium tartrate by utilizing the asymmetric habit of their crystals (Gal, 2008, 2013; Pasteur, 1848; Tobe, 2003). He also discovered the change in optical rotation induced by the different structures of the enantiomers in water solution. The discovery of enantiomers has played an important role in advancing the scientific understanding of molecular chirality.

The only effective method of establishing the absolute configuration of molecules, by assessing the anomalous scattering in an X-ray diffraction experiment, was proposed by Bijvoet et al. (1951). Thereafter, the absolute crystal structures of L- and D-tartaric acid were determined to be monoclinic with space group *P*2<sub>1</sub> by Stern and Beevers

(1950), and by Okaya et al. (1966), respectively. However, the exact crystal structure of L-tartaric acid, including the positions of all hydrogen atoms, has not yet been determined. As reported in recently published papers, the crystal structures of monohydrate D-tartaric and monohydrate racemic (MDL-) tartaric acid were determined by means of single-crystal X-ray diffraction (Nie et al., 2001; Song et al., 2006). However, the positions of all hydrogen atoms in MDL-tartaric acid have not been refined (Nie et al., 2001). These structures are very different from those of anhydrate L- and D-tartaric acid described in previous papers (Okaya et al., 1966; Stern & Beevers, 1950).

The purpose of this study is to determine the exact crystal structures of L(+)-tartaric, D(-)-tartaric, and MDL-tartaric acid, including the positions of all hydrogen atoms, at room temperature using X-ray diffraction measurements and to report the thermal properties of these acid crystals by differential scanning calorimetry (DSC) and thermogravimetric-differential thermal analysis (TG-DTA) measurements.

## 2. Experimental

### 2.1 Crystal Growth

Single crystals of L(+)-tartaric and D(-)-tartaric acid were grown at room temperature by slow evaporation from aqueous solutions in a desiccator over P<sub>2</sub>O<sub>5</sub>. DL-tartaric acid crystals were also grown by the same method in air under ambient conditions at room temperature. The solution used for DL-tartaric acid crystals was prepared from a solution of L-tartaric acid sealed in an autoclave and maintained at 448 K for 48 hours. Some of the acid in the sealed solution was converted to D-tartaric acid. The DL-tartaric acid, which consists of 50% L-tartaric and 50% D-tartaric acid, has a lower solubility in water than L- and D-tartaric acid. Thus, the growth of DL-tartaric acid crystals from the solution was more rapid than that of L- or D-tartaric acid crystals.

### 2.2 X-ray Crystal Structure Determination

The X-ray diffraction measurements were carried out using a Rigaku Saturn CCD X-ray diffractometer with graphite-monochromated Mo K<sub>α</sub> radiation ( $\lambda = 0.71073 \text{ \AA}$ ). The diffraction data were collected at 299 K using an  $\omega$  scan mode with a crystal-to-detector distance of 40 mm, and processed using the CrystalClear software package. The samples used were spherical with diameters of 0.32–0.38 mm. The intensity data were corrected for Lorentz polarization and absorption effects. The crystal structures were solved with direct methods using the SIR2011 program and refined on  $F^2$  by full-matrix least-squares methods using the SHELXL-2013 program in the WinGX package (Burla et al., 2012; Farrugia, 2012; Sheldrick, 2015).

### 2.3 Thermal Measurements

DSC and TG-DTA measurements were respectively carried out in the temperature ranges of 105–380 K and 300–760 K, using DSC7020 and TG-DTA7300 systems from Seiko Instruments Inc. Aluminum open pans with no pan cover were used as the measuring vessels and reference pans for the DSC and TG-DTA measurements. Fine powder samples prepared from crushed single crystals were used for the measurements. The sample amount varied between 3.22 and 7.04 mg, and the heating rates were 5 or 10 K min<sup>-1</sup> under a dry nitrogen gas flow.

## 3. Results and Discussion

### 3.1 Crystal Structures

The crystal structures of L(+)-tartaric, D(-)-tartaric, and DL-tartaric acid were determined at room temperature by X-ray diffraction. The lattice parameters calculated from all observed reflections for L- and D-tartaric acid indicated that both crystals belong to a monoclinic system. The systematic extinctions in the observed reflections revealed that the possible space group of both acids is  $P2_1$  or  $P2_1/m$ . Furthermore, the intensity statistics of the reflections strongly indicated that the crystals belong to an acentric point group. Thus, the space groups of L- and D-tartaric acid were determined to be monoclinic  $P2_1$ . The lattice parameters calculated from all observed reflections for DL-tartaric acid indicated that the crystal belongs to a triclinic system. The intensity statistics strongly revealed that the crystal belongs to a centric point group. Thus, the space group of DL-tartaric acid was determined to be triclinic  $P\bar{1}$ .

The atomic coordinates and thermal parameters for these acid crystals, including the positions of all hydrogen atoms, were determined at room temperature. The observed crystal of DL-tartaric acid in this work was confirmed to be monohydrate racemic (MDL-) tartaric acid, C<sub>4</sub>H<sub>6</sub>O<sub>6</sub>·H<sub>2</sub>O. Final *R*-factors of 2.80%, 2.82%, and 4.73% for L-tartaric, D-tartaric, and MDL-tartaric acid, respectively, were calculated for 2619, 2703, and 3162 unique observed reflections. The relevant crystal data, as well as a summary of the intensity data collection, and structure refinement parameters are given in Table 1. The positional parameters in fractions of a unit cell, and the thermal parameters are listed in Table 2. Selected bond lengths (in Å) and angles (in degrees) are given in Table 3. The hydrogen-bond geometry (in Å and degrees) is presented in Table 4.

Figure 1 shows the projections of the crystal structures of L- and D-tartaric acid along the *b*-axis at room temperature.

The observed structures of L- and D-tartaric acid, including the positions of all hydrogen atoms, are almost the same as that of D-tartaric acid described by Okaya et al. (1966). The observed structure of D-tartaric acid is very different from that of monohydrate D-tartaric acid crystal (orthorhombic  $P2_12_12_1$ ) reported by Song et al. (2006). Although analyses of their structure indicate that an additional water molecule is present in D-tartaric acid, the water molecule is not present in the structure of D-tartaric acid used in this study and in the previous paper (Okaya et al., 1966). The single crystals of D-tartaric acid reported by Song et al. (2006) were grown by the slow cooling method by reducing the temperature from 343 K. The sample crystals used in this study were grown by the slow evaporation method at room temperature. Therefore, it is considered that the difference in water molecules between the D-tartaric acid crystals is caused by the difference in crystal growth conditions.

Table 1. Crystal data, intensity collection and structure refinement for (a) L-tartaric acid ( $C_4H_6O_6$ ), (b) D-tartaric acid ( $C_4H_6O_6$ ), and (c) MDL-tartaric acid (monohydrate racemic tartaric acid,  $C_4H_6O_6 \cdot H_2O$ ) crystals at room temperature.

	(a) L-tartaric acid	(b) D-tartaric acid	(c) MDL-tartaric acid
Compound	$C_4H_6O_6$	$C_4H_6O_6$	$C_4H_6O_6 \cdot H_2O$
$M_r$	150.09	150.09	168.10
Crystal shape, color	Plate, colorless	Plate, colorless	Prism, colorless
Crystal system, space group	Monoclinic, $P2_1$	Monoclinic, $P2_1$	Triclinic, $P\bar{1}$
Lattice constants	$a = 7.7230(6) \text{ \AA}$ $b = 6.0056(3) \text{ \AA}$ $c = 6.2134(4) \text{ \AA}$	$a = 7.7281(5) \text{ \AA}$ $b = 6.0025(3) \text{ \AA}$ $c = 6.2113(4) \text{ \AA}$	$a = 4.8701(4) \text{ \AA}$ $b = 8.0586(8) \text{ \AA}$ $c = 9.1550(10) \text{ \AA}$ $\alpha = 109.289(3)^\circ$ $\beta = 99.846(3)^\circ$ $\gamma = 96.104(2)^\circ$
$V, Z$	$283.65(3) \text{ \AA}^3, 2$	$283.63(3) \text{ \AA}^3, 2$	$328.97(6) \text{ \AA}^3, 2$
D(cal.)	$1.757 \text{ Mg m}^{-3}$	$1.757 \text{ Mg m}^{-3}$	$1.697 \text{ Mg m}^{-3}$
$\mu(\text{Mo } K_\alpha)$	$0.173 \text{ mm}^{-1}$	$0.173 \text{ mm}^{-1}$	$0.169 \text{ mm}^{-1}$
$F(000)$	156	156	176
Sample shape	Sphere	Sphere	Sphere
Size in diameter	$2r = 0.36 \text{ mm}$	$2r = 0.32 \text{ mm}$	$2r = 0.38 \text{ mm}$
$\theta$ range for data collection	$3.33 - 37.74^\circ$	$3.33 - 37.86^\circ$	$2.42 - 37.92^\circ$
Index ranges	$-13 \leq h \leq 13$ $-10 \leq k \leq 10$ $-10 \leq l \leq 10$	$-13 \leq k \leq 13$ $-10 \leq k \leq 10$ $-10 \leq k \leq 10$	$-8 \leq l \leq 8$ $-13 \leq l \leq 13$ $-15 \leq l \leq 15$
Reflections collected	8176	8151	9411
Unique	2911 [ $R(\text{int})=0.0236$ ]	2955 [ $R(\text{int})=0.0213$ ]	3393 [ $R(\text{int})=0.0273$ ]
Completeness to $\theta_{\text{max}}$	97.2 %	97.6 %	95.3 %
Absorption correction type	Spherical	Spherical	Spherical
Transmission factor $T_{\text{min}}-T_{\text{max}}$	0.8614 – 0.8625	0.8614 – 0.8625	0.8614 – 0.8625
Date [ $I > 2\sigma(I)$ ]	2619	2703	3162
Parameter	116	116	133
Final $R$ indices	$R_1 = 0.0280$ $wR_2 = 0.0673$	$R_1 = 0.0282$ $wR_2 = 0.0743$	$R_1 = 0.0473$ $wR_2 = 0.1189$
$R$ indices (all data)	$R_1 = 0.0317$ $wR_2 = 0.0689$	$R_1 = 0.0316$ $wR_2 = 0.0765$	$R_1 = 0.0508$ $wR_2 = 0.1217$
Factors $a$ and $b$ in weighting*	$a = 0.0369, b = 0$	$a = 0.0445, b = 0$	$a = 0.0489, b = 0.0647$
Goodness-of-fit on $F^2$	1.012	1.038	1.109
Extinction coefficient	0.158(17)	0.134(19)	0.177(18)
Largest diff. peak and hole	0.263, -0.199 $e\text{\AA}^{-3}$	0.245, -0.196 $e\text{\AA}^{-3}$	0.454, -0.347 $e\text{\AA}^{-3}$
Flack parameter	-0.1(3)	0.0(3)	

\*Weighting scheme  $w = 1/[\sigma^2(F_o^2) + (aP)^2 + bP]$ ,  $P = (F_o^2 + 2F_c^2)/3$

Table 2. Atomic coordinates and thermal parameters ( $\times 10^4 \text{ \AA}^2$ ) at room temperature for (a) L-tartaric acid, (b) D-tartaric acid, and (c) MDL-tartaric acid crystals with standard deviations in brackets. The anisotropic thermal parameters are defined as  $\exp[-2\pi^2 (U_{11}a^{*2}h^2 + U_{22}b^{*2}k^2 + U_{33}c^{*2}l^2 + 2U_{23}b^*c^*kl + 2U_{13}a^*c^*hl + 2U_{12}a^*b^*hk)]$ . The isotropic thermal parameters ( $\text{\AA}^2$ ) for H atoms are listed under  $U_{11}$ .

Atom	$x$	$Y$	$z$	$U_{11}$	$U_{22}$	$U_{33}$	$U_{23}$	$U_{13}$	$U_{12}$
<b>(a) L-tartaric acid</b>									
C(1)	0.0217(1)	0.4564(2)	0.2500(2)	142(4)	302(5)	217(4)	6(3)	47(3)	-21(3)
C(2)	0.2003(1)	0.4808(2)	0.1811(2)	133(3)	239(4)	179(4)	1(3)	41(3)	0(3)
C(3)	0.2941(1)	0.6928(2)	0.2824(2)	145(3)	230(4)	221(4)	-22(3)	61(3)	-7(3)
C(4)	0.4635(1)	0.7145(2)	0.1906(2)	169(3)	208(3)	246(4)	-21(3)	75(3)	-29(3)
O(1)	-0.0774(1)	0.6283(2)	0.1801(2)	165(3)	454(5)	450(5)	154(4)	116(3)	86(3)
O(2)	-0.0215(1)	0.3009(2)	0.3499(2)	279(4)	433(5)	522(6)	171(5)	188(4)	-13(4)
O(3)	0.30657(9)	0.2902(1)	0.2341(1)	196(3)	251(3)	225(3)	-15(3)	55(2)	30(3)
O(4)	0.3378(1)	0.6748(2)	0.5104(1)	231(3)	412(4)	205(3)	-73(3)	72(3)	-17(3)
O(5)	0.4293(1)	0.7414(2)	-0.0221(1)	232(3)	463(5)	251(3)	50(3)	100(3)	-50(3)
O(6)	0.60889(9)	0.7012(2)	0.3009(1)	152(3)	414(4)	314(4)	-56(4)	60(3)	-23(3)
H(1)	-0.167(3)	0.620(4)	0.232(3)	0.059(6)					
H(2)	0.339(2)	0.282(3)	0.375(3)	0.030(4)					
H(3)	0.247(3)	0.703(4)	0.560(3)	0.049(5)					
H(4)	0.530(2)	0.748(4)	-0.082(3)	0.045(5)					
H(5)	0.179(2)	0.496(3)	0.028(2)	0.020(3)					
H(6)	0.221(2)	0.825(3)	0.234(2)	0.017(3)					
<b>(b) D-tartaric acid</b>									
C(1)	0.4785(1)	0.4347(2)	0.2502(2)	142(3)	307(5)	213(4)	8(3)	46(3)	-18(3)
C(2)	0.2996(1)	0.4103(2)	0.3188(1)	132(3)	240(4)	177(3)	-1(3)	38(2)	-3(3)
C(3)	0.2058(1)	0.1982(2)	0.2175(2)	147(3)	231(4)	219(3)	-19(3)	62(2)	-8(3)
C(4)	0.0365(1)	0.1766(2)	0.3094(2)	173(3)	206(3)	242(4)	-20(3)	76(3)	-30(3)
O(1)	0.5775(1)	0.2626(2)	0.3199(2)	167(3)	460(5)	446(5)	157(4)	114(3)	87(3)
O(2)	0.5215(1)	0.5905(2)	0.1502(2)	280(4)	434(5)	519(6)	171(5)	189(4)	-15(4)
O(3)	0.19333(9)	0.6010(1)	0.2658(1)	195(3)	254(3)	222(3)	-13(2)	54(2)	33(3)
O(4)	0.1623(1)	0.2163(2)	-0.0105(1)	230(3)	415(5)	197(3)	-70(3)	69(2)	-11(3)
O(5)	0.0708(1)	0.1497(2)	0.5224(1)	233(3)	467(5)	245(3)	49(3)	98(3)	-54(3)
O(6)	-0.10885(9)	0.1899(2)	0.1991(1)	154(3)	416(4)	310(4)	-54(3)	58(2)	-24(3)
H(1)	0.668(3)	0.268(4)	0.267(3)	0.049(6)					
H(2)	0.160(2)	0.609(3)	0.126(3)	0.030(4)					
H(3)	0.251(2)	0.185(4)	-0.063(3)	0.042(5)					
H(4)	-0.030(3)	0.140(4)	0.579(3)	0.048(5)					
H(5)	0.320(2)	0.396(3)	0.471(3)	0.024(3)					
H(6)	0.280(2)	0.065(3)	0.267(2)	0.018(3)					
<b>(c) MDL-tartaric acid</b>									
C(1)	0.3471(2)	-0.2953(1)	0.10734(9)	278(3)	228(3)	233(3)	41(2)	82(2)	96(2)
C(2)	0.2171(2)	-0.1335(1)	0.18337(9)	260(3)	227(3)	236(3)	62(2)	74(2)	108(2)
C(3)	0.4410(2)	0.0373(1)	0.24760(9)	276(3)	230(3)	250(3)	64(2)	100(2)	107(2)
C(4)	0.3078(2)	0.1980(1)	0.3221(1)	306(3)	207(3)	310(4)	79(3)	123(3)	94(2)
O(1)	0.5115(2)	-0.2696(1)	0.0164(1)	488(4)	281(3)	404(4)	61(3)	272(3)	124(3)
O(2)	0.2909(2)	-0.43576(9)	0.1294(1)	518(4)	260(3)	471(4)	132(3)	271(3)	182(3)
O(3)	0.0959(1)	-0.16165(9)	0.30456(8)	300(3)	290(3)	327(3)	113(2)	158(2)	149(2)
O(4)	0.6667(1)	0.0229(1)	0.35914(8)	283(3)	349(3)	285(3)	29(2)	53(2)	149(2)
O(5)	0.1053(2)	0.2210(1)	0.22026(9)	432(4)	312(3)	357(3)	105(3)	100(3)	208(3)
O(6)	0.3878(2)	0.2889(1)	0.46123(9)	503(4)	333(3)	338(3)	-3(3)	81(3)	194(3)
O(7)	0.8819(2)	0.4944(1)	0.3164(1)	543(5)	310(3)	546(5)	159(3)	290(4)	210(3)
H(1)	0.563(6)	-0.382(4)	-0.039(3)	0.107(9)					
H(2)	-0.050(4)	-0.103(2)	0.319(2)	0.052(4)					
H(3)	0.668(4)	0.090(3)	0.448(2)	0.065(6)					
H(4)	0.030(5)	0.324(3)	0.268(3)	0.075(6)					
H(5)	0.077(3)	-0.125(2)	0.096(2)	0.031(3)					
H(6)	0.508(3)	0.055(2)	0.158(2)	0.029(3)					
H(7)	0.801(5)	0.539(3)	0.396(3)	0.076(6)					
H(8)	0.977(5)	0.586(3)	0.308(3)	0.080(7)					

Table 3. Selected interatomic distances (in Å) and angles (in degrees) for (a) L-tartaric acid, (b) D-tartaric acid, and (c) MDL-tartaric acid crystals at room temperature.

(a) L-tartaric acid			
O(1)–C(1)	1.313(1)	O(2)–C(1)	1.201(1)
O(3)–C(2)	1.413(1)	O(4)–C(3)	1.401(1)
O(5)–C(4)	1.311(1)	O(6)–C(4)	1.210(1)
C(1)–C(2)	1.522(1)	C(2)–C(3)	1.543(1)
C(3)–C(4)	1.523(1)		
O(1)–C(1)–O(2)	125.73(9)	O(1)–C(1)–C(2)	109.61(8)
O(2)–C(1)–C(2)	124.65(9)	C(1)–C(2)–O(3)	111.98(8)
C(1)–C(2)–C(3)	110.37(8)	O(3)–C(2)–C(3)	111.22(7)
C(2)–C(3)–O(4)	111.15(8)	C(2)–C(3)–C(4)	106.87(7)
O(4)–C(3)–C(4)	108.43(7)	C(3)–C(4)–O(5)	110.77(8)
C(3)–C(4)–O(6)	123.69(9)	O(5)–C(4)–O(6)	125.50(8)
(b) D-tartaric acid			
O(1)–C(1)	1.313(1)	O(2)–C(1)	1.201(1)
O(3)–C(2)	1.414(1)	O(4)–C(3)	1.401(1)
O(5)–C(4)	1.313(1)	O(6)–C(4)	1.211(1)
C(1)–C(2)	1.524(1)	C(2)–C(3)	1.543(1)
C(3)–C(4)	1.522(1)		
O(1)–C(1)–O(2)	125.79(9)	O(1)–C(1)–C(2)	109.67(8)
O(2)–C(1)–C(2)	124.53(9)	C(1)–C(2)–O(3)	112.05(8)
C(1)–C(2)–C(3)	110.47(8)	O(3)–C(2)–C(3)	111.16(7)
C(2)–C(3)–O(4)	111.10(8)	C(2)–C(3)–C(4)	106.89(7)
O(4)–C(3)–C(4)	108.46(7)	C(3)–C(4)–O(5)	110.76(8)
C(3)–C(4)–O(6)	123.73(9)	O(5)–C(4)–O(6)	125.47(9)
(c) MDL-tartaric acid			
O(1)–C(1)	1.298(1)	O(2)–C(1)	1.225(1)
O(3)–C(2)	1.412(1)	O(4)–C(3)	1.409(1)
O(5)–C(4)	1.310(1)	O(6)–C(4)	1.210(1)
C(1)–C(2)	1.520(1)	C(2)–C(3)	1.535(1)
C(3)–C(4)	1.520(1)		
O(1)–C(1)–O(2)	124.94(7)	O(1)–C(1)–C(2)	113.54(7)
O(2)–C(1)–C(2)	121.50(7)	C(1)–C(2)–O(3)	108.53(6)
C(1)–C(2)–C(3)	110.55(6)	O(3)–C(2)–C(3)	111.63(6)
C(2)–C(3)–O(4)	110.25(7)	C(2)–C(3)–C(4)	109.97(6)
O(4)–C(3)–C(4)	110.55(7)	C(3)–C(4)–O(5)	112.48(7)
C(3)–C(4)–O(6)	121.03(8)	O(5)–C(4)–O(6)	126.48(8)

Table 4. Hydrogen bond distances (in Å) and angles (in degrees) for (a) L-tartaric acid, (b) D-tartaric acid, and (c) MDL-tartaric acid crystals at room temperature.

D–H···A	D–H	H···A	D···A	<D–H···A
(a) L-tartaric acid				
O(1)–H(1)···O(6) <sup>(a)</sup>	0.82(2)	1.92(2)	2.696(1)	159(2)
O(3)–H(2)···O(6) <sup>(b)</sup>	0.87(2)	2.04(2)	2.897(1)	168(2)
O(4)–H(3)···O(2) <sup>(c)</sup>	0.83(2)	2.01(2)	2.836(1)	173(2)
O(5)–H(4)···O(3) <sup>(d)</sup>	0.92(2)	1.73(2)	2.633(1)	169(2)
C(2)–H(5)	0.94(2)			
C(3)–H(6)	0.99(1)			
(b) D-tartaric acid				
O(1)–H(1)···O(6) <sup>(e)</sup>	0.83(2)	1.90(2)	2.696(1)	161(2)
O(3)–H(2)···O(6) <sup>(f)</sup>	0.86(2)	2.05(2)	2.896(1)	168(2)
O(4)–H(3)···O(2) <sup>(g)</sup>	0.83(2)	2.01(2)	2.836(1)	172(2)
O(5)–H(4)···O(3) <sup>(h)</sup>	0.92(2)	1.73(2)	2.632(1)	168(2)
C(2)–H(5)	0.94(2)			
C(3)–H(6)	1.00(2)			
(c) MDL-tartaric acid				
O(1)–H(1)···O(2) <sup>(i)</sup>	0.96(3)	1.72(3)	2.6789(9)	171(2)
O(3)–H(2)···O(4) <sup>(j)</sup>	0.90(2)	1.82(2)	2.7123(9)	177(2)
O(4)–H(3)···O(6)	0.82(2)	2.20(2)	2.6539(9)	115(2)
O(4)–H(3)···O(3) <sup>(k)</sup>	0.82(2)	2.21(2)	2.881(1)	140(2)
O(5)–H(4)···O(7) <sup>(l)</sup>	0.95(2)	1.59(2)	2.524(1)	170(2)
O(7)–H(7)···O(6) <sup>(l)</sup>	0.88(2)	1.99(2)	2.823(1)	158(2)
O(7)–H(8)···O(3) <sup>(m)</sup>	0.86(2)	2.07(2)	2.899(1)	162(2)
C(2)–H(5)	0.99(1)			
C(3)–H(6)	0.98(1)			

Symmetry codes: (a)  $x-1, y, z$ , (b)  $-x+1, y-1/2, -z+1$ , (c)  $-x, y+1/2, -z+1$ , (d)  $-x+1, y+1/2, -z$ , (e)  $x+1, y, z$ , (f)  $-x, y+1/2, -z$ , (g)  $-x+1, y-1/2, -z$ , (h)  $-x, y-1/2, -z+1$ , (i)  $-x+1, -y-1, -z$ , (j)  $x-1, y, z$ , (k)  $-x+1, -y, -z+1$ , (l)  $-x+1, -y+1, -z+1$ , (m)  $x+1, y+1, z$ .

The crystal structures of L- and D-tartaric acid are related by mirror symmetry, as shown in Fig. 1. The intramolecular bond lengths and angles in the  $C_4H_6O_6$  molecule, and the hydrogen bond lengths and angles between adjacent  $C_4H_6O_6$  molecules, for L-tartaric acid are almost the same as those for D-tartaric acid, respectively, as shown in Tables 3 and 4. The angle between the two least-squares planes of atoms C(1)C(2)O(1)O(2)O(3) and C(3)C(4)O(4)O(5)O(6) for L-tartaric acid was calculated to be  $56.33(5)^\circ$ , whereas that for D-tartaric acid was calculated to be  $56.34(5)^\circ$ . The structures of both acids consist of hydrogen-bonded networks, which are formed by four different types of O–H–O hydrogen bonds between adjacent  $C_4H_6O_6$  molecules, forming layers parallel to the  $ac$ -plane. Thus, it is concluded that the crystal structure of L-tartaric acid is almost exactly the same as that of D-tartaric acid.

Figure 2 shows the projection of the MDL-tartaric acid crystal structure along the  $a$ -axis at room temperature. The positional parameters of all atoms in the MDL-tartaric acid crystal, including the positions of all hydrogen atoms, were determined in this study. The observed structure is almost the same as that reported by Nie et al. (2001). There is one bound water molecule in the structure of MDL-tartaric acid, which is different from the structures of L- and D-tartaric acid, as mentioned above. There are five different types of O–H–O hydrogen bonds in the structure, forming layers parallel to the  $bc$ -plane and chains along the  $a$ -axis. The layers of hydrogen-bonded networks consist of an O(1)–H(1)···O(2) hydrogen bond between adjacent  $C_4H_6O_6$  molecules, and O(5)–H(4)···O(7)–H(7)···O(6) and O(5)–H(4)···O(7)–H(8)···O(3) bonds between two  $C_4H_6O_6$  and  $H_2O$  molecules, as shown in Fig. 2. Moreover, the chains along the  $a$ -axis consist of O(3)–H(2)···O(4) and O(4)–H(3)···O(3) hydrogen bonds between  $C_4H_6O_6$  molecules. These

hydrogen-bonded networks are also very different from those in the structures of L- and D-tartaric acid. The angle between the two least-squares planes of atoms C(1)C(2)O(1)O(2)O(3) and C(3)C(4)O(4)O(5)O(6) for MDL-tartaric acid was calculated to be  $72.79(4)^\circ$ . The intramolecular bond lengths and angles in the  $C_4H_6O_6$  molecule of MDL-tartaric acid are very similar to those of L- and D-tartaric acid, as shown in Table 4. However, the value of the angle is widely different from those of L- and D-tartaric acid [ $56.33(5)^\circ$  and  $56.34(5)^\circ$ , respectively], and the torsion in the molecule of MDL-tartaric acid is larger than those of L- and D-tartaric acid. When the single crystals of MDL-tartaric acid were kept under low humidity, the crystal surface exhibited chalky white opacities. It is considered that the white opacities on the crystal surface are caused by the breaking of hydrogen bonds, followed by water evaporation from the crystal surface.

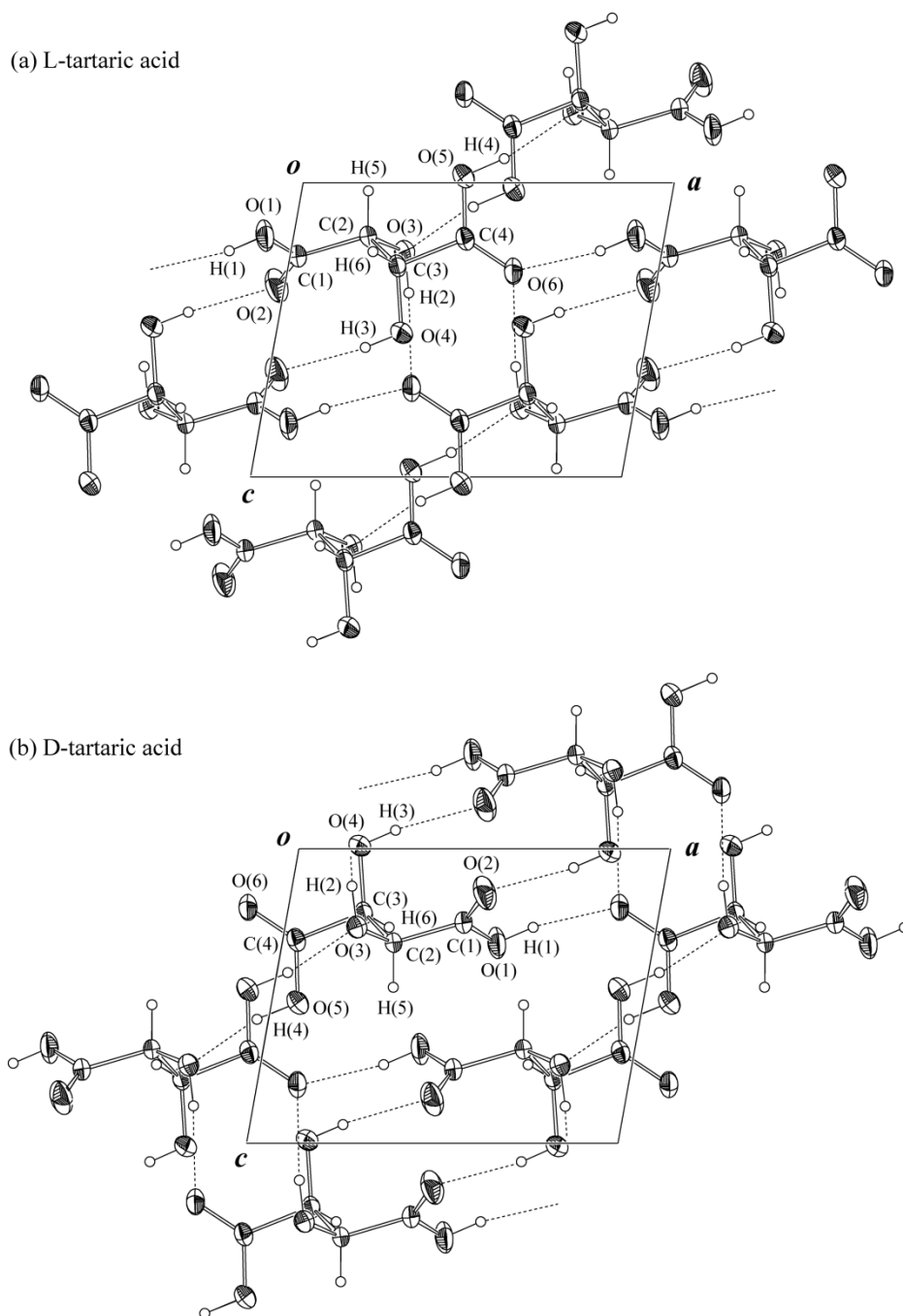


Figure 1. Projections of the crystal structures of (a) L-tartaric and (b) D-tartaric acid along the *b*-axis at room temperature with 50% probability-displacement thermal ellipsoids. The dashed short lines show O–H···O hydrogen bonds, as shown in Table 4.

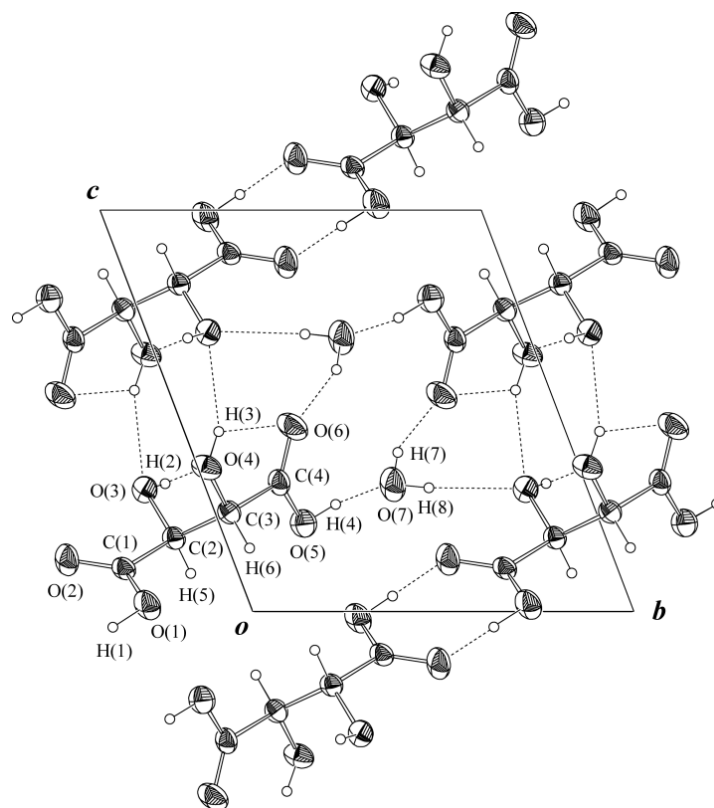


Figure 2. Projection of the crystal structure of MDL-tartaric acid along the  $a$ -axis at room temperature with 50% probability-displacement thermal ellipsoids. The dashed short lines show O–H $\cdots$ O hydrogen bonds, as shown in Table 4.

### 3.2 Thermal Analyses

Figure 3 shows the DSC curve of MDL-tartaric acid upon heating in the temperature range from 105 to 380 K. The weight of the sample (powder) used for the measurement was 4.36 mg, and the heating rate was 5 K min<sup>-1</sup> under a dry nitrogen gas flow of 40 ml min<sup>-1</sup>. A large endothermic peak is clearly seen in the DSC curve at 321.2 K, with an onset temperature of 306.1 K. The transition enthalpy,  $\Delta H$ , and transition entropy,  $\Delta S$ , associated with the large peak were determined to be 47.6 kJ mol<sup>-1</sup> and 18.7R, respectively, where R is the gas constant (8.314 JK<sup>-1</sup>mol<sup>-1</sup>). Moreover, no significant endothermic or exothermic peaks were observed in the DSC curves of L- and D-tartaric acid in the temperature range of 105–380 K. Generally, it is believed that a clear peak in the DSC curve is attributed to a change of exchange energy at phase transition. Thus, these results indicate that the transition of MDL-tartaric acid takes place at 306.1 K, and there is no phase transition of L- and D-tartaric acid in the temperature range between 105 and 380 K. Table 5 shows the peak temperature, onset temperature (transition temperature),  $\Delta H$ , and  $\Delta S$  obtained from the DSC curve. Owing to the presence of structurally bound water molecules in MDL-tartaric acid mentioned above, it is expected that the large endothermic peak at 321.2 K is caused by the evaporation of the water. Furthermore, a very small endothermic peak is seen in the DSC curve at 272 K, as shown in Fig. 3. We confirmed that a small endothermic peak (~0.5 mW) is observed at 260 K in the DSC curve, representing the solution (weight of 0.73 mg) of MDL-tartaric acid used for the growth medium. Thus, the small peak observed at 272 K in MDL-tartaric acid is considered to be derived from aqueous-solution infiltration into the sample crystal.

Figure 4 shows the TG, differential TG (DTG), and DTA curves for L-tartaric, D-tartaric, and MDL-tartaric acid crystals in the temperature range of 300–760 K. The weights of the samples (powder) of L-tartaric, D-tartaric, and MDL-tartaric acid used for the measurements were 6.60, 5.82, and 6.51 mg, respectively, and the heating rates were 10 K min<sup>-1</sup> under a dry nitrogen gas flow of 300 ml min<sup>-1</sup>. The DTA curve for L-tartaric acid exhibited one large endothermic peak at 444.2 K and two rather small endothermic peaks at 496.9 and 532.1 K. The D-tartaric acid crystal also showed one large and two small endothermic peaks at 444.6, 495.5, and 529.4 K. Moreover, peaks in the DTG curve of L-tartaric acid were seen at 444.3, 493.2, and 531.0 K, and those of D-tartaric acid were seen at 444.5, 496.5, and 528.7 K. The onset temperatures of the large endothermic peaks in the DTA curves of L- and D-tartaric acid were determined to be 443.0 and 443.2 K, respectively. The endothermic peaks in the DTA curve of both acids correspond to

the peaks in the DTG curve, respectively. The DTG curve, which is the first derivative of the TG curve, reveals the temperature dependence of the rate of weight loss. Therefore, the endothermic peaks on the DTA curve are associated with the rate of weight loss on the TG curve due to thermal decomposition of the sample.

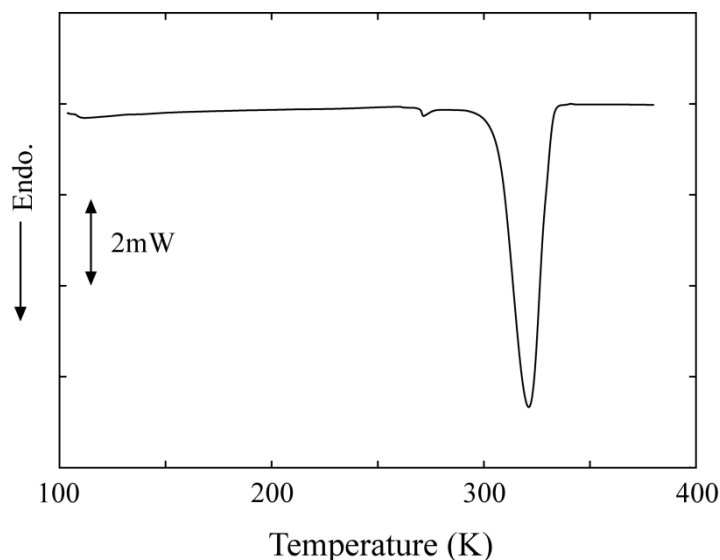


Figure 3. DSC curve for MDL-tartaric acid crystal on heating. The sample weight (powder) was 4.36 mg, and the heating rate was 5 K min<sup>-1</sup> under a dry N<sub>2</sub> gas flow of 40 ml min<sup>-1</sup>.

Table 5. Peak temperatures, onset temperatures (transition temperatures), transition enthalpy  $\Delta H$ , and transition entropy  $\Delta S$  for (a) L-tartaric acid, (b) D-tartaric acid, and (c) MDL-tartaric acid crystals obtained from DSC, DTA, and DTG curves.

(a) L-tartaric acid	DTA	Peak temp. (K)	444.2	496.9	532.1	
		Onset temp. (K)	443.0			
	DTG	Peak temp. (K)	444.3	493.2	531.0	
(b) D-tartaric acid	DTA	Peak temp. (K)	444.6	495.5	529.4	
		Onset temp. (K)	443.2			
	DTG	Peak temp. (K)	444.5	496.5	528.7	
(c) MDL-tartaric acid	DSC	Peak temp. (K)	321.2			
		Onset temp. (K)	306.1			
		$\Delta H$ (kJ mol <sup>-1</sup> )	47.6			
		$\Delta S/R$	18.7			
	DTA	Peak temp. (K)	324.2	483.8	511.7	526.1
		Onset temp. (K)	313.1	480.6		
	DTG	Peak temp. (K)	322.8	483.7	513.3	525.5

Gas constant  $R = 8.314 \text{ JK}^{-1}\text{mol}^{-1}$

The DTA curve of MDL-tartaric acid exhibited two large endothermic peaks at 324.2 and 483.8 K and two small endothermic peaks at 511.7 and 526.1 K. The DTG curve of MDL-tartaric acid has peaks at 322.8, 483.7, 513.3, and 525.5 K, and these DTG peaks correspond to the respective DTA peaks. The observed DTA peak at 324.2 K corresponds to the above-mentioned DSC peak at 321.2 K. The slight difference of 3 K between the peak temperatures is probably caused by differences in heating rate (5 or 10 K min<sup>-1</sup>) and start temperature (105 or 300 K) for the measurements. The onset temperatures of the two large endothermic peaks at 324.2 and 483.8 K were determined to be 313.1 and 480.6 K, respectively. The peak at 324.2 K was not observed in the DSC and DTA curves of L- and D-tartaric acid. The start temperature of the weight loss (onset temperature of 480.6 K) in the TG curve of MDL-tartaric acid is

higher than those of L- and D-tartaric acid (443.0 or 443.2 K, respectively), as shown in Fig. 4 and Table 5. This temperature of MDL-tartaric acid is approximately 40 K higher than those of L- and D-tartaric acid. The end temperatures (approximately 550 K) of the weight loss of the three acids are approximately same, as shown in the TG curves of Fig. 4. The temperature range of the weight loss in L- and D-tartaric acid is 88 and 85 K, respectively, and in MDL-tartaric acid is 42 K. This range of MDL-tartaric acid is thus approximately half those of L- and D-tartaric acid. The results indicate that the MDL-tartaric acid crystal at high temperature is thermally more stable than the L- and D-tartaric acid crystals.

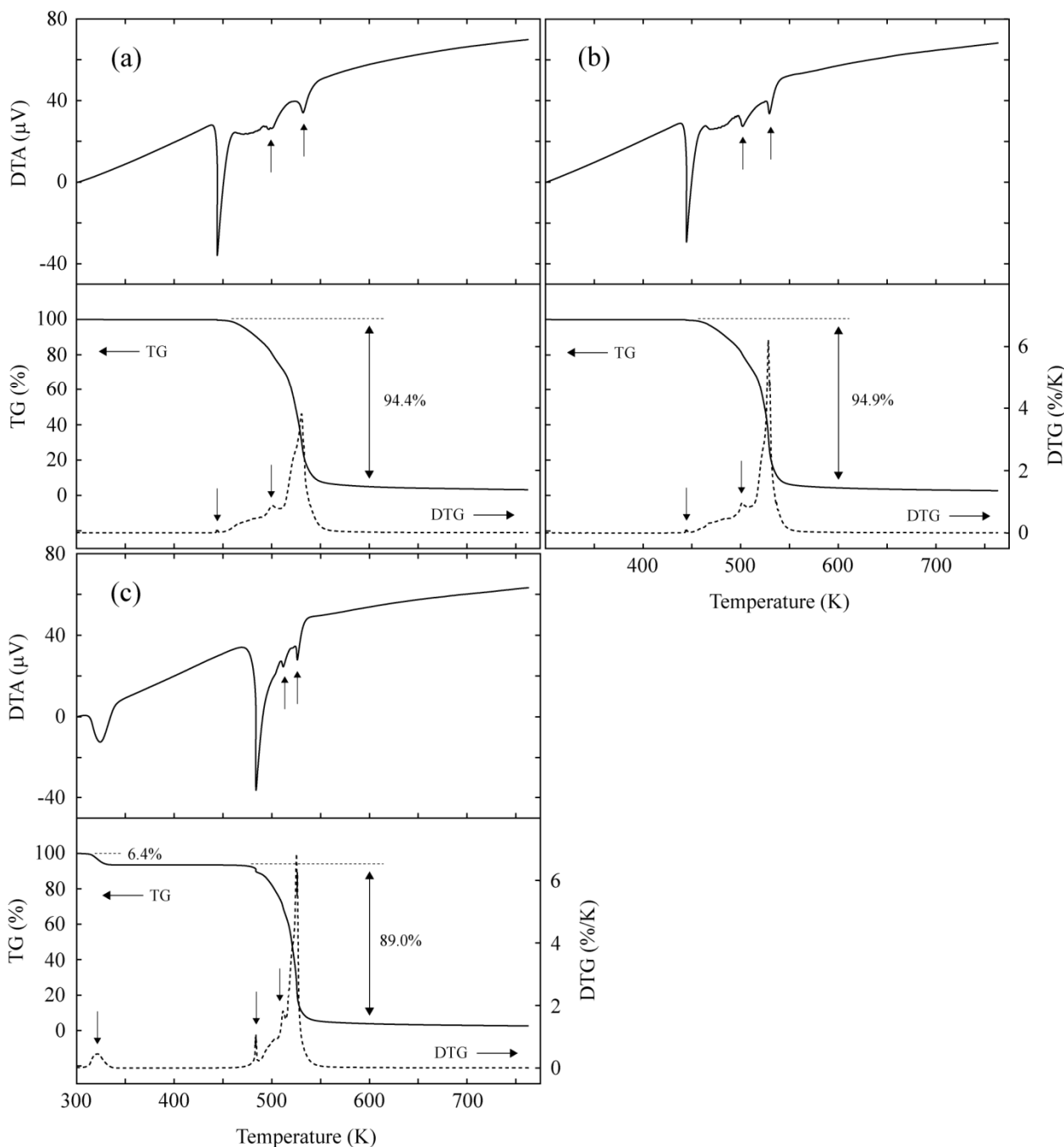


Figure 4. TG, DTG, and DTA thermograms for (a) L-tartaric acid, (b) D-tartaric acid, and (c) MDL-tartaric acid crystals on heating. The sample weights (powder) for (a), (b), and (c) curves were 6.60, 5.82, and 6.51 mg, respectively. The heating rates were  $10 \text{ K min}^{-1}$  under a dry  $\text{N}_2$  gas flow of  $300 \text{ ml min}^{-1}$ .

The weight losses of L- and D-tartaric acid around 440 K were determined to be 94.4% and 94.9%, respectively, from the TG curves in the temperature range of 425–575 K, as shown in Fig. 4. We assume that the weight loss is caused by

the evolution of  $3\text{H}_2\text{O}$  and  $3\text{CO}$  gases due to thermal decomposition of the sample (which is the chemical formula of  $\text{C}_4\text{H}_6\text{O}_6$ ). The theoretical weight loss is calculated to be 92.0%  $[(3 \times 18.02 + 3 \times 28.01) / 150.09]$ . This value is very close to the experimental weight losses of 94.4% and 94.9%. One of four carbon atoms in the  $\text{C}_4\text{H}_6\text{O}_6$  molecule remains in the sample pan by the evolution of  $3\text{H}_2\text{O}$  and  $3\text{CO}$  gases from the sample. After measurements, the inside of the sample pans for L- and D-tartaric acid was confirmed to change from silver to black in color.

The weight loss around 320 K of MDL-tartaric acid was determined to be 6.4% from the TG curve, and it was also determined to be 89.0% around 480 K in the temperature range of 475–575 K. As mentioned above, it is expected that the endothermic peak at 324.2 K is caused by the evaporation of bound water molecules from the sample (which is the chemical formula of  $\text{C}_4\text{H}_6\text{O}_6 \cdot \text{H}_2\text{O}$ ). The theoretical weight loss caused by the elimination of one  $\text{H}_2\text{O}$  molecule is calculated to be 10.7%  $[=18.02/168.10]$ . We assume that the weight loss around 480 K for MDL-tartaric acid is the same as those of L- and D-tartaric acid, as mentioned above. Thus, the theoretical weight loss in the temperature range of 475–575 K is calculated to be 82.1%  $[(3 \times 18.02 + 3 \times 28.01) / 168.10]$ . The theoretical weight loss value of 10.7% is much larger than the experimental weight loss of 6.4%, and conversely, one of 82.1% is slightly smaller than the experimental weight loss of 89.0%. Then, we assume that one-half of bound water molecules, which is one of two crystallographically equivalent water molecules in the unit cell, evaporates around 320 K, and the remaining water contributes to the value of the weight loss by the evolution of  $3\text{H}_2\text{O}$  and  $3\text{CO}$  gases around 480 K. The theoretical weight loss around 320 K is calculated to be 5.4%  $[=0.5 \times 18.02 / 168.10]$ , and that in the temperature range of 475–575 K is 87.5%  $[(0.5 \times 18.02 + 3 \times 18.02 + 3 \times 28.01) / 168.10]$ . These values calculated are very close to the experimental weight losses of 6.4% and 89.0%, respectively. One of four carbon atoms in MDL-tartaric acid at high temperature remains in the sample pan, as similar to those in L- and D-tartaric acid by decomposition. After the measurement for MDL-tartaric acid, the inside of the sample pan was confirmed to change from silver to black in color too.

### 3.3 Relation between Water Evaporation and Hydrogen-bonding Properties

As mentioned above, at room temperature, the O(7) atom in the bound  $\text{H}_2\text{O}$  molecule of MDL-tartaric acid forms two hydrogen bonds of  $\text{O}(7)\text{--H}(7)\cdots\text{O}(6)$  and  $\text{O}(7)\text{--H}(8)\cdots\text{O}(3)$  with the  $\text{C}_4\text{H}_6\text{O}_6$  molecule, as shown in Table 4 and Fig. 2. The lengths of these hydrogen bonds are 2.823(1) and 2.899(1) Å, respectively, and the H atom involved in the bonds is attached to the O(7) atom. Moreover, the O(5) atom in the  $\text{C}_4\text{H}_6\text{O}_6$  molecule forms the  $\text{O}(5)\text{--H}(4)\cdots\text{O}(7)$  hydrogen bond with the O(7) atom in the  $\text{H}_2\text{O}$  molecule. The hydrogen bond length is 2.524(1) Å, and is significantly shorter than those of  $\text{O}(7)\text{--H}(7)\cdots\text{O}(6)$  and  $\text{O}(7)\text{--H}(8)\cdots\text{O}(3)$ . It is known that the O–H–O hydrogen bond has a double-minimum potential well along the coordinate of proton motion when the  $\text{O}\cdots\text{O}$  distance in a hydrogen bond is in the range of 2.43–2.65 Å (Fukami et al., 2010, 2014; Ichikawa, 2000). In fact, the distance of the  $\text{O}(5)\cdots\text{O}(7)$  bond is within the range of 2.43–2.65 Å. Moreover, a difference electron density peak of  $0.12 \text{ e}\text{\AA}^{-3}$  at the final stage of refinement was found close to the O(7) atom on the hydrogen bond, and the peak position was observed at the distance of 0.79 Å from the O(7) atom. The H(4) atom involved in the  $\text{O}(5)\text{--H}(4)\cdots\text{O}(7)$  hydrogen bond is attached to the O(5) atom. These findings indicate that the  $\text{O}(5)\text{--H}(4)\cdots\text{O}(7)$  hydrogen bond has an asymmetric double-minimum potential well along the  $\text{O}\cdots\text{O}$  bond.

Here, it is expected that the rate of proton transfer between two possible sites on the  $\text{O}(5)\text{--H}(4)\text{--O}(7)$  hydrogen bond increases with increasing temperature. When the H(4) atom in the hydrogen bond is located at the O(7) site, the H atom is attached to the O(7) atom. Then, one of hydrogen atoms (H(7) or H(8)) in the  $\text{H}_2\text{O}$  molecule is removed from the O(7) atom due to the so-called “ice rules”. The  $\text{H}_2\text{O}$  molecule forms the shorter  $\text{O}(7)\text{--H}(4)\cdots\text{O}(5)$  hydrogen bond between the  $\text{H}_2\text{O}$  and  $\text{C}_4\text{H}_6\text{O}_6$  molecules by the exchange of hydrogen partners. Since the hydrogen-bonding strength is mainly influenced by  $\text{O}\cdots\text{O}$  distance of the bond, the hydrogen bond strength between the  $\text{H}_2\text{O}$  and  $\text{C}_4\text{H}_6\text{O}_6$  molecules is increased by the exchange of the hydrogen bonds. As the result, the evaporation of  $\text{H}_2\text{O}$  molecules will certainly be reduced by increasing the bonding strength. The evolution of the weight loss corresponding to 50% bound water molecules due to the evaporation around 320 K mentioned above, indicates that the exchange of the hydrogen bonds in one-half of water molecules takes place at the temperature, and that is, the relative occupancies of the two sites for the H(4) atom are estimated to be  $\sim 0.5$ . The occupancy of  $\sim 0.5$  at each site means that the double-minimum potential well of the  $\text{O}(5)\text{--H}(4)\text{--O}(7)$  hydrogen bond is changed from asymmetric to symmetric with increasing temperature. It is concluded that the difference between the evaporation temperatures of 306.1 and 480.6 K for bound water molecules is caused by the physical properties of the  $\text{O}(5)\text{--H}(4)\cdots\text{O}(7)$  hydrogen bond.

## 4. Conclusion

Single crystals of L(+)-tartaric, D(–)-tartaric, and racemic tartaric acid were grown at room temperature by slow evaporation from aqueous solutions. The exact room-temperature crystal structures of L-tartaric, D-tartaric and racemic tartaric acid, including the positions of all hydrogen atoms, respectively, were determined to be monoclinic with space group  $P2_1$ , monoclinic with space group  $P2_1$ , and triclinic with space group  $P\bar{1}$ , by means of single-crystal X-ray diffraction. The observed structures of L- and D-tartaric acid were almost exactly the same as each other, and very

similar to those reported in the previous papers (Okaya et al., 1966; Stern & Beevers, 1950). The grown single crystals of racemic tartaric acid in this study were monohydrate racemic (MDL-) tartaric acid,  $C_4H_6O_6 \cdot H_2O$ , and very similar to that reported in the previous paper (Nie et al, 2001). Moreover, one of the O–H–O hydrogen bonds in the acid was 2.524(1) Å in length, and was suggested to have the asymmetric double-minimum potential well along the coordinate of proton motion at room temperature.

The weight losses due to thermal decomposition of L- and D-tartaric acid occurred at 443.0 and 443.2 K, respectively, and those in MDL-tartaric acid occurred at 306.1 and 480.6 K. The weight losses for L- and D-tartaric acid were caused by the evolution of  $3H_2O$  and  $3CO$  gases due to decomposition, and the losses at 306.1 and 480.6 K for MDL-tartaric acid were caused by the evaporation of one-half bound water molecules and by the remaining water molecules and the evolution of  $3H_2O$  and  $3CO$  gases, respectively. The weight losses of MDL-tartaric acid are related to the physical properties of the O–H–O hydrogen bond having the proton transfer between two possible sites in the double-minimum potential well along the O··O bond, and one of four carbon atoms in the  $C_4H_6O_6$  molecule of these acids remains in the sample pans upon heating to 575 K for the decomposition reactions.

## References

- Abdel-Kader, M. M., El-Kabbany, F., Taha, S., Abosehly, A. M., Tahoon, K. K., & El-Sharkawy, A. A. (1991). Thermal and electrical properties of ammonium tartrate. *J. Phys. Chem. Solids*, 52(5), 655-658. <http://www.sciencedirect.com/science/journal/00223697/52/5>
- Bijvoet, J. M., Peerdeman, A. F., & Bommel, A. J. (1951). Determination of the absolute configuration of optically active compounds by means of X-rays. *Nature*, 168, 271-272. <http://dx.doi.org/10.1038/168271a0>
- Boese, R., & Heinemann, O. (1993). Crystal structure of calcium tartrate tetrahydrate,  $C_4H_4O_6Ca(H_2O)_4$ . *Z. Kristallogr.*, 205(1-2), 348-349. <http://dx.doi.org/10.1524/zkri.1993.205.12.348>
- Bootsma, G. A., & Schoone, J. C. (1967). Crystal structures of mesotartaric acid. *Acta Crystallogr.*, 22(4), 522-532. <http://dx.doi.org/10.1107/S0365110X67001070>
- Burla, M. C., Caliandro, R., Camalli, M., Carrozzini, B., Cascarano, G. L., Giacovazzo, C., Mallamo, M., Mazzone, A., Polidori, G., & Spagna, R. (2012). SIR2011: a new package for crystal structure determination and refinement. *J. Appl. Crystallogr.*, 45(2), 357-361. <http://dx.doi.org/10.1107/S0021889812001124>
- Buschmann, J., & Luger, P. (1985). Structure of potassium hydrogen (+)-tartrate at 100 K,  $K^+ \cdot C_4H_5O_6^-$ . *Acta Crystallogr.*, C41(2), 206-208. <http://dx.doi.org/10.1107/S0108270185003341>
- Derewenda, Z. S. (2008). On wine, chirality and crystallography. *Acta Crystallogr.*, A64(1), 246-258. <http://dx.doi.org/10.1107/S0108767307054293>
- Desai, C. C., & Patel, A. H. (1988). Crystal data for ferroelectric  $RbHC_4H_4O_6$  and  $NH_4HC_4H_4O_6$  crystals. *J. Mater. Sci. Lett.*, 7(4), 371-373. <http://link.springer.com/article/10.1007/BF01730747>
- Farrugia, L. J. (2012). WinGX and ORTEP for Windows: an update. *J. Appl. Crystallogr.*, 45(4), 849-854. <http://dx.doi.org/10.1107/S0021889812029111>
- Firdous, A., Quasim, I., Ahmad, M. M., & Kotru, P. N. (2010). Dielectric and thermal studies on gel grown strontium tartrate pentahydrate crystals. *Mull. Mater. Sci.*, 33(4), 377-382. <http://www.ias.ac.in/maternal/bmsaug2010/377.pdf>
- Fukami, T., Miyazaki, J., Tomimura, T., & Chen, R. H. (2010). Crystal structures and isotope effect on  $Na_5H_3(SeO_4)_4 \cdot 2H_2O$  and  $Na_5D_3(SeO_4)_4 \cdot 2D_2O$  crystals. *Cryst. Res. Technol.*, 45(8), 856-862. <http://dx.doi.org/10.1002/crat.201000116>
- Fukami, T., Tahara, S., & Nakasone, K. (2014). Thermal properties and structures of  $CsHSO_4$  and  $CsDSO_4$  crystals. *Int. Res. J. Pure Appl. Chem.*, 4(6), 621-637. <http://dx.doi.org/10.9734/IRJPAC/2014/11331>
- Gal, J. (2008). The discovery of biological enantioselectivity: Louis Pasteur and the fermentation of tartaric acid, 1857 - a review and analysis 150 yr later. *Chirality*, 20(1), 5-19. <http://dx.doi.org/10.1002/chir.20494>
- Gal, J. (2013). Citation for chemical breakthrough awards: Choosing pasteur's award-winning publication. *Bull. Hist. Chem.*, 38(1), 7-12. <http://www.scs.illinois.edu/~mainzv/HIST/awards/Citations/v38-1%20p7-12.pdf>
- Hawthorne, F. C., Borys, I., & Ferguson, R. B. (1982). Structure of calcium tartrate tetrahydrate. *Acta Crystallogr.*, B38(9), 2461-2463. <http://dx.doi.org/10.1107/S0567740882009042>
- Ichikawa, M. (2000). Hydrogen-bond geometry and its isotope effect in crystals with OHO bonds - revisited. *J. Mol. Struct.*, 552(1-3), 63-70. [http://dx.doi.org/doi:10.1016/S0022-2860\(00\)00465-8](http://dx.doi.org/doi:10.1016/S0022-2860(00)00465-8)
- Lowry, T. M. (1923). Pasteur as chemist. *Proc. Roy. Soc. Med.*, 16, 16-20.

<http://www.ncbi.nlm.nih.gov/pmc/articles/PMC2104002/>

- Nie, J. J., Xu, D. J., Wu, J. Y., & Chiang, M. Y. (2001). Redetermination of racemic tartaric acid monohydrate. *Acta Crystallogr.*, *E57*(5), o428-o429. <http://dx.doi.org/10.1107/S1600536801006158>
- Okaya, Y., Stemple, N. R., & Kay, M. I. (1966). Refinement of the structure of D-tartaric acid by X-ray and neutron diffraction. *Acta Crystallogr.*, *21*(2), 237-243. <http://dx.doi.org/10.1107/S0365110X66002664>
- Parry, G. S. (1951). The crystal structure of hydrate racemic acid. *Acta Crystallogr.*, *4*(2), 131-138. <http://dx.doi.org/10.1107/S0365110X51000416>
- Pasteur, M. L. (1848). Sur les relations qui peuvent exister la forme cristalline, la composition chimique et Le sens de la polarisation rotatoire. *Ann. Chim. Phys.*, *24*, 442-463. <http://gallica.bnf.fr/ark:/12148/bpt6k65691733/f446.image.r=Annales%20de%20chimie%20et%20de%20physique.langEN>
- Sheldrick, G. M. (2015). Crystal structure refinement with SHELXL. *Acta Crystallogr.*, *C71*(1), 3-8. <http://dx.doi.org/10.1107/S2053229614024218>
- Song, Q. B., Teng, M. Y., Dong, Y., Ma, C. A., & Sun, J. (2006). (2S,3S)-2,3-Dihydroxy-succinic acid monohydrate. *Acta Crystallogr.*, *E62*(8), o3378-o3379. <http://dx.doi.org/10.1107/S1600536806021738>
- Stern, F., & Beevers, C. A. (1950). The crystal structure of tartaric acid. *Acta Crystallogr.*, *3*(5), 341-346. <http://dx.doi.org/10.1107/S0365110X50000975>
- Tobe, Y. (2003). The reexamination of Pasteur's experiment in Japan. *Mendeleev Commun.*, *13*(3), 93-94. <http://dx.doi.org/10.1070/MC2003v013n03ABEH001803>
- Torres, M. E., Peraza, J., Yanes, A. C., López, T., Stockel, J., López, D. M., Solans, X., Bocanegra, E., & Silgo, G. G. (2002). Electrical conductivity of doped and undoped calcium tartrate. *J. Phys. Chem. Solids*, *63*(4), 695-698. <http://www.sciencedirect.com/science/journal/00223697/63/4>

## Copyrights

Copyright for this article is retained by the author(s), with first publication rights granted to the journal.

This is an open-access article distributed under the terms and conditions of the Creative Commons Attribution license (<http://creativecommons.org/licenses/by/3.0/>).